Influence of an elongational flow field on random coil and rod-like polymers in solution

D. G. Peiffer, M. W. Kim and R. D. Lundberg
Exxon Research and Engineering Company, Clinton Township–Route 22 East
Annandale, New Jersey 08801, USA
(Received 19 July 1985)

The conformational response and spatial arrangement of random coil and rod-like macromolecules in solution was investigated utilizing an opposing jet device. This device is capable of generating a well-defined elongational flow field, which is quite useful for probing intra- and intermolecular interactions of sulphonated polystyrene (random coil) and xanthan (rod-like chain). With regard to the random coil in an aqueous environment, it was determined that its behaviour below the critical overlap concentration (C^*) follows the anticipated trends as predicted by theory. Above C^*, the elongational behaviour is determined by the intermolecular entanglement structure. However, changes in the ionic strength in these latter solutions reverts behaviour to that observed below C^*. One implication of this finding is briefly discussed. Interestingly, intermolecular interactions dominate the behaviour of rod-like polymers, such as xanthan, below and above C^*. Superimposed on these interactions is the subtle influence of the flow field both outside and along the axis connecting the centre of the jets. These results confirm that the xanthan macromolecule behaves as a liquid crystal at all concentrations investigated, even with relatively large changes in ionic strength.

(Keywords: extensional flow; opposing jet apparatus; birefringence; sulphonated polystyrene; xanthan)

INTRODUCTION

There are a number of well-established techniques for studying the molecular characteristics and behaviour of individual macromolecules in solution. Static and dynamic light scattering, neutron scattering, colligative property-based methods and viscometry are the most widely used techniques. In many instances, viscometry is the method of choice, since measurements can be made *in-situ* without special preparation. For example, valuable information is obtained on solutions where light cannot penetrate or where selective deuterium labelling is synthetically difficult. Furthermore, the technique can uniquely probe the rheological response of the polymeric fluid mixture with changes in solvent quality, temperature and, in particular, shear rate. An interesting aspect of these viscosity–shear rate measurements is that the flow field possesses a large rotational component in which the coiled chains experience only minor excursions from this conformation[1]. Irrespective of the relatively small changes in coil dimensions, many properties of polymeric fluid can be measured and understood by assuming that the fluid elements experience little, if any, extensional behaviour. However, there is growing interest in flows exhibiting a significant elongational component, since probing the extensional behaviour of a chain can lead to a better understanding of the inter- and intramolecular interactions in macromolecular systems. This could undoubtedly contribute to the increased usefulness of these materials in a myriad of applications such as high tensile strength fibres and films[2–5], antimisting agents[6,7] and drag reduction additives[8].

A particularly intriguing aspect of this latter flow field is that the polymer chains can be deformed to high extension ratios. When the chain is an isolated entity in the solution system, then it can be shown from both a theoretical[9–11] and experimental[12–16] viewpoint that complete extension of the random coil is possible. According to theory, the elongational viscosity will rapidly rise with the elongational deformation rate, then tends to saturate at a specific large value when the elongation rate exceeds the inverse of the molecular relaxation time. In more qualitative terms, the macromolecules are pulled out into an ellipsoidal shape under the influence of a pure elongational flow field, and when the strain rate exceeds the effective restoring force, the chain expands as far as possible. This idealized picture becomes somewhat blurred, since it is likely the effective restoring forces vary as the chain expands. Thus, the expansion is anticipated to occur quite rapidly, but not in an instantaneous manner. Therefore, the residence time of the fluid elements should be long enough for the required extension to be achieved. This so-called coil to rod-like transition sets in when

$$\tau\dot{\varepsilon}_c = 1 \qquad (1)$$

where $\dot{\varepsilon}_c$ is the critical elongational shear rate for this transition and τ is the longest relaxation time of the chain in question. τ is the relaxation time associated with the mechanical response of the random coil to a small deformation and is not associated with the time required to elongate fully the chain[12,16]. Physically, this implies that the initial deformation of the coil is the rate-determining step in the transition.

Experimentally, it has been shown that the above theoretical requirements are satisfied if the experiments are carried out, for example, by blowing or sucking polymer solutions through narrow opposing orifices or jets[13–16]. With regard to suction-driven flow, a well-defined elongational flow field exists along a symmetry line connecting the centres of the opposing jets. In this

0032-3861/86/040493-10$03.00

device, the elongational strain rate ($\dot{\varepsilon}$) and the molecular residence time are of sufficient magnitude that the molecules subjected to it experience high chain extension along the symmetry axis.

Following the lead of Keller and coworkers[13-16], we briefly describe in the present work our results on the influence of an elongational flow field on two water-soluble polymeric materials: fully sulphonated polystyrene and the polysaccharide, xanthan. The elongational flow field is generated through an opposing jet device built in our laboratory. This apparatus, in conjunction with a polarizing microscope, is capable of measuring the extent of molecular orientation as $\dot{\varepsilon}$ is varied and simultaneously photographing the complex flow patterns for later evaluation. Presently, we are able to generate $\dot{\varepsilon}$ up to approximately $15000\,s^{-1}$ in low viscosity fluids. Our results confirm these extensional velocity gradients are of sufficient magnitude and duration significantly to influence the conformation and spatial arrangement (i.e. orientation) of our two model systems: a random coil (sulphonated polystyrene) and a rod-like macromolecule (xanthan).

This approach, as will be presented in a future publication, gives us a sensitive probe with regard to the intra- and intermolecular interactions of individual polymer chains and how these interactions are modulated with changes in solvent environment and polymer concentration.

EXPERIMENTAL

The apparatus used in this work is shown schematically in *Figure 1*. The separation of the two jets is 0.11 cm, and the jet radius is 0.022 cm. The flow rate of the solution through the jets is controlled by means of a vacuum pump and a flow valve connected to a relatively large solution trap reservoir. In all instances, only single pass measurements were made so as to avoid possible molecular degradation effects.

In general, the presence of birefringence along the axis connecting the centres of the jets is directly related to the deformation and alignment of macromolecules subjected to elongational shear stresses. This observation is well documented in the literature[13]. The polymer solution, contained in the opposing jet device, is situated between the crossed polarizer and analyser. The jet axis is placed at 45° to both polars. A quarter-wave plate is inserted into the light beam after the device, which enables the intensity of the retardation to be measured by the classical method of Senarmont. In order to obtain birefringence values, the retardation is divided by the thickness of the birefringent region located along a symmetry axis joining the two jets. This thickness could not be determined very rigorously due to the relatively diffuse nature of the birefringent region. Interestingly, addition of small increments of sodium chloride to sodium styrenesulphonate solutions allowed for a relatively clear view of the region exhibiting maximum retardation.

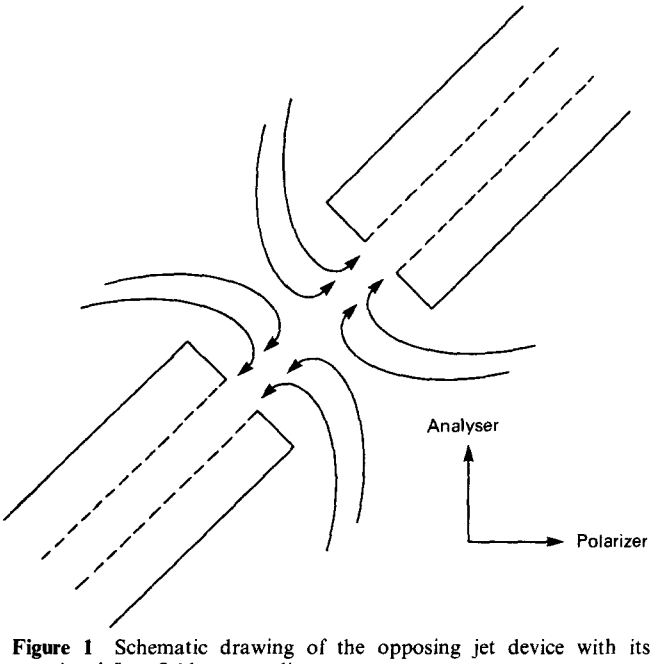

Figure 1 Schematic drawing of the opposing jet device with its associated flow field contour lines

In these two-component solutions, the form birefringence was evaluated in order to determine whether the observed birefringence was due primarily to the intrinsic orientation of the polymer chains or simply due to the anisotropic distribution of the chains in a solvent possessing a different refractive index, i.e. form birefringence. It is quite reasonable to assume that at the maximum measured birefringence, the chains in a dilute solution are completely elongated within the elongational flow field. We applied the theory of Wiener[18] for parallel rods at the appropriate polymer concentration and found the predicted form birefringence values are of the order of 10–15% of the experimental birefringence values. Therefore, the birefringence values can be correlated, to a good approximation, to the inherent orientation of the chains.

The materials used in this study were fully sulphonated sodium neutralized polystyrene (Versa T1600—National Starch Co.) and a xanthan gum (Kelco Corp.). Both samples were polydispersed with the average molecular weight of the former material given as approximately 6×10^6, while the latter polymer was estimated[17] to be about 2×10^6 with rod lengths of between 0.2 and 2.0 μm. These two polymers are of interest, since the sulphonated polystyrene has a random coil conformation and is especially sensitive to changes in ionic strength, while xanthan possesses a rod-like conformation which remains invariant with changes in ionic strength. The xanthan solutions were prepared according to the procedure of Jamieson *et al.*[19].

The shear viscosity measurements are performed with a Low Shear 30 from Contraves (Switzerland) at controlled temperature (25°C).

RESULTS AND DISCUSSION

Random coil polymers

It is well known that high molecular weight polyelectrolytes are very effective viscosity enhancers in aqueous solutions. These materials become especially effective as the polymer concentration is reduced. This is due, in part, to the dissociation of the counterions from the vicinity of the chain backbone. At this stage, repulsive interactions become increasingly larger than the constrictive entropic restoring forces allowing for an enlargement in the hydrodynamic volume. Interestingly, the coil dimensions are very sensitive to subtle changes in the concentration of dissolved salts, since the hydrated

anions and cations are capable of shielding these repulsive forces. A direct consequence of this interaction is a reduction in the solution viscosity. An example of this behaviour is presented in *Figure 2*, where the shear viscosity profiles of several fresh and salt water solutions containing sulphonated polystyrene are shown as a function of shear rate. As anticipated, salt has a marked influence on viscosity and, in addition, these solutions at all polymer and salt levels examined show shear thinning behaviour in this rotational type flow field. The viscosity at higher shear rates in fresh water solutions is approximately an order of magnitude lower than at low rates of shear. This decrease can be viewed as a consequence of the net decrease in entanglement density induced by the flow field[20]. Moreover, it is evident from these data and from previous studies[22,23] that the transition from Newtonian to pseudoplastic behaviour occurs in the low shear rate range and depends on polymer concentration, temperature and ionic strength for a particular polymer solution. The transition typically shifts to higher shear rates as the temperature is increased, concentration is decreased, salt level is increased or molecular weight is varied. However, significant deviations from the random coil conformation are not expected in this type of flow configuration as compared to an elongational flow field.

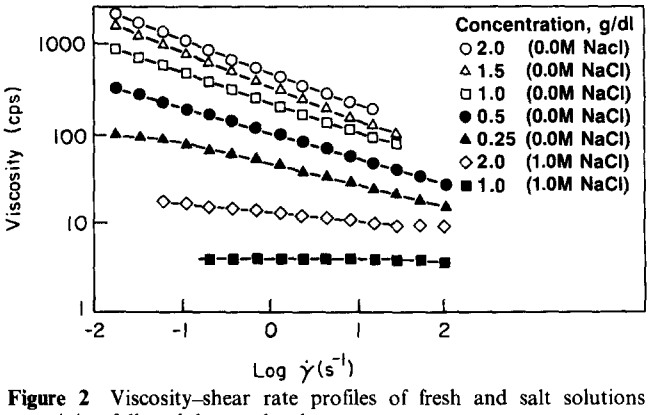

Figure 2 Viscosity–shear rate profiles of fresh and salt solutions containing fully sulphonated polystyrene

The influence of an elongational flow field produced in an opposing jet device on a sulphonated polystyrene solution is shown in *Figure 3*. It is immediately apparent at very low extensional velocity gradients ($< 40\ s^{-1}$) that the field of view is dark and lacks any discernible structure, as seen through cross polars (not shown). As the elongational shear rate is increased, however, birefringence begins to be observed, indicating that coiled chains are being oriented. As expected, the birefringence is steadily enhanced as the flow rate is increased, eventually reaching a limiting value (the qualitative aspects of this phenomenon are observed in *Figure 3*). These observations parallel the work by Keller *et al.* on the flow birefringence measurements on a series of monodispersed sulphonated polystyrenes[16].

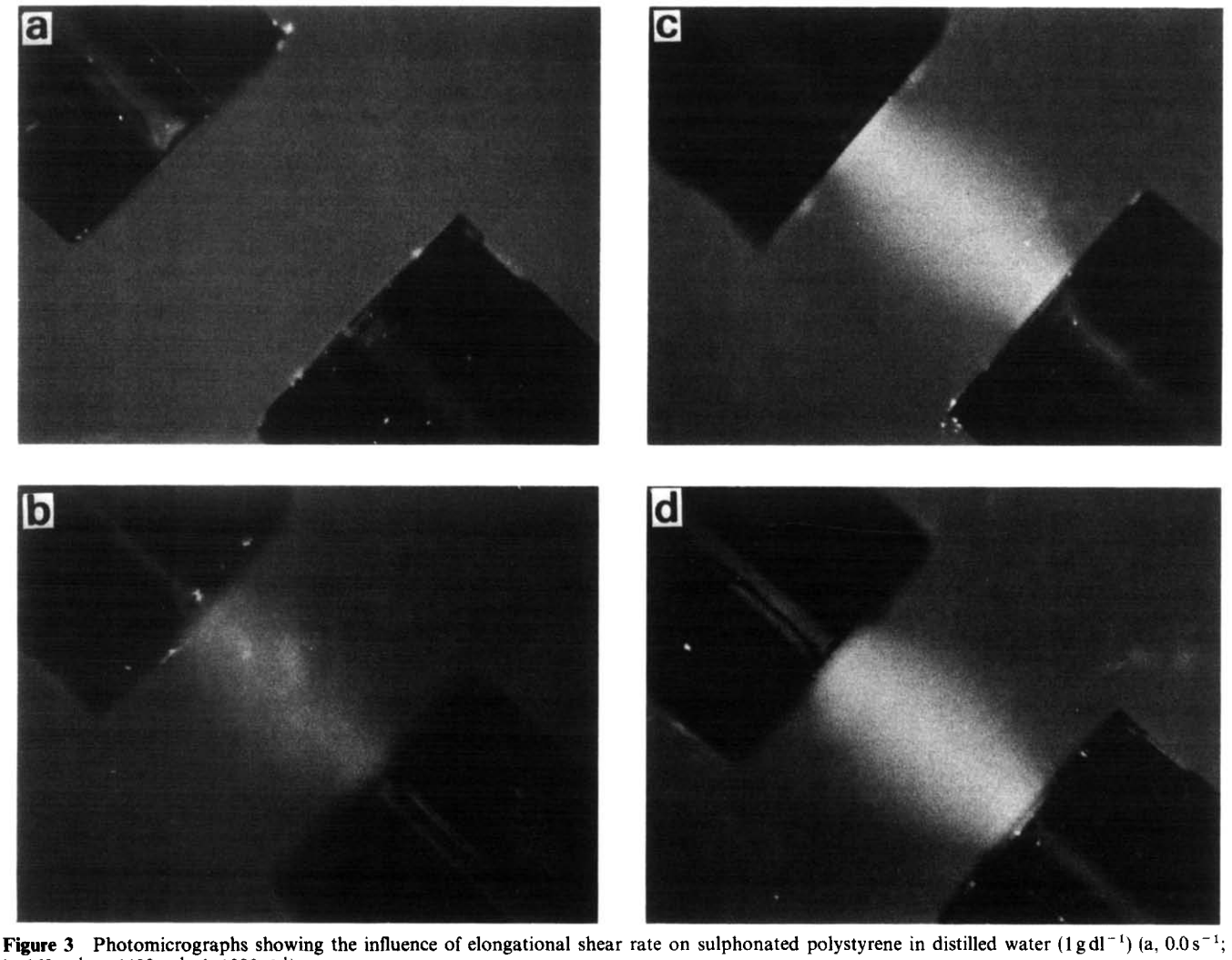

Figure 3 Photomicrographs showing the influence of elongational shear rate on sulphonated polystyrene in distilled water ($1\ g\ dl^{-1}$) (a, $0.0\ s^{-1}$; b, $160\ s^{-1}$; c, $1100\ s^{-1}$; d, $1200\ s^{-1}$)

A direct consequence of this flow field on polymer behaviour is the marked concentration dependence of the retardation on the elongational shear rate. This is shown in *Figure 4*, where the polymer concentration is varied from dilute to the semidilute regimes. Dilute solution behaviour occurs between 0.25 and 0.5 g dl^{-1} in these fresh water solutions for this polyelectrolyte. In the very dilute solution regime, the retardation rises quite rapidly after a specific critical elongational shear rate, $\dot{\varepsilon}_c$, is approached. Following a relatively short excursion along $\dot{\varepsilon}$, the retardation becomes saturated. This is typical behaviour predicted by theory for macromolecules that are completely isolated entities in an elongational flow field. Interestingly, however, the retardation becomes increasingly broadened as the concentration is enhanced and, in fact, becomes easily measurable at rather low $\dot{\varepsilon}$ and only begins to approach saturation, at least within the flow rate limitations of our apparatus. It is expected the retardation will begin to level out in significantly higher flow fields if the molecular weight of the chains is not significantly degraded. These results are intriguing, since it is apparent that intermolecular interactions have a dramatic effect on the orientability of the individual chains, due, in part, to the fact that the physical entanglements do not allow the chains sufficient time to disentangle. As a consequence, the entanglements prohibit the chains from extending to their maximum extent. Rather, it becomes easier to orient short segments within an individual chain. A schematic representation of this effect is presented in *Figure 5*. In dilute solution, full chain extension is achievable, but becomes increasingly difficult as more entanglements are introduced into the solution through changes in polymer concentration. It is noted that these entangled chains have markedly different relaxation times from their unentangled counterparts. Thus, according to equation (1), this should be reflected in broader retardations–$\dot{\varepsilon}$ curves, as indeed is the case. That is, as the relaxation times become increasingly lengthened, $\dot{\varepsilon}_c$ will shorten by a corresponding amount.

The data of *Figure 4* are replotted in *Figure 6* with the retardation and its associated birefringence calculated on a 100% polymer concentration. Again, it is shown in the dilute solution regime, a $\dot{\varepsilon}_c$ is required prior to a very sharp rise in birefringence associated with the extension of the polymer chain. The birefringence value at the saturation limit corresponds approximately to a fully aligned chain as confirmed from independent literature sources, i.e. flow birefringence measurements[22].

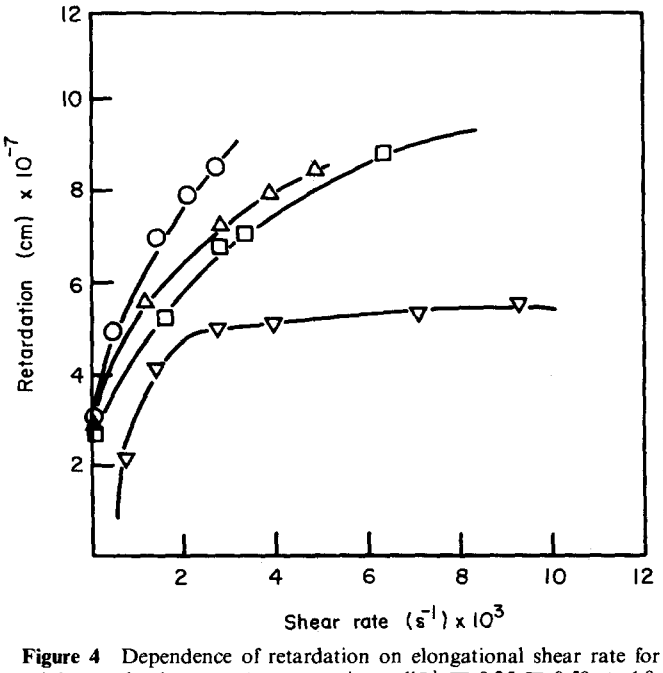

Figure 4 Dependence of retardation on elongational shear rate for sulphonated polystyrene (concentration, g dl^{-1}: ▼, 0.25; □, 0.50; △, 1.0; ○, 2.0) in distilled water solution

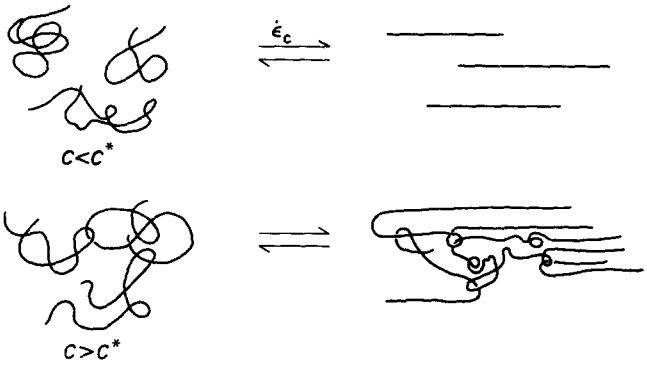

Figure 5 Schematic drawing showing the behaviour of flexible chains below and above C^* in an elongational flow field

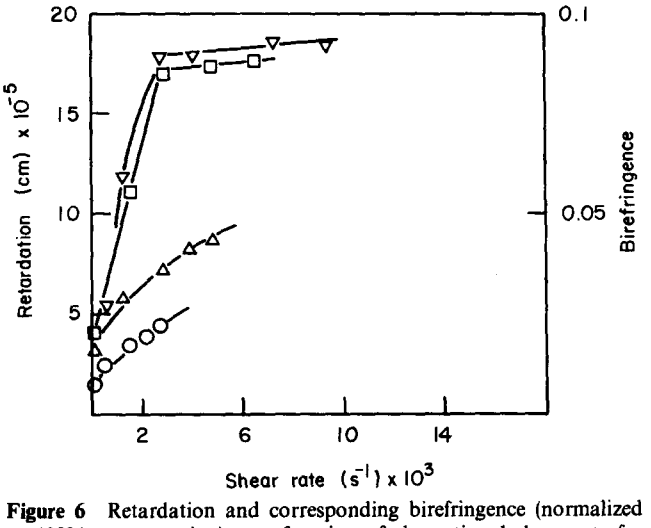

Figure 6 Retardation and corresponding birefringence (normalized to 100% concentration) as a function of elongational shear rate for sulphonated polystyrene (concentration, g dl^{-1}: ▽, 0.25; □, 0.50; △, 1.0; ○, 2.0) in distilled water solution

As noted previously, in the semidilute solution regime, a broadening of relaxation times takes place due to physical entanglements. Even though the segments of the chains between entanglements can become highly oriented, complete alignment is not possible, as reflected in the lower birefringence values at a specific $\dot{\varepsilon}$. At the present time, it is not possible to determine if the higher molecular weight components of the distribution have a disproportionate influence on this entanglement structure. Experiments are presently being performed in order to determine whether these long contour length chains significantly influence behaviour, especially in their interactions with lower molecular weight species, and will be reported on in the very near future.

Influence of salt water

As noted previously, the rheological characteristics of sulphonated polystyrene in aqueous solution are markedly reduced with relatively small variations in ionic strength. This phenomenon is directly related to a reduction in hydrodynamic volume of the polymer chain. It is of interest, however, to examine whether this change in chain

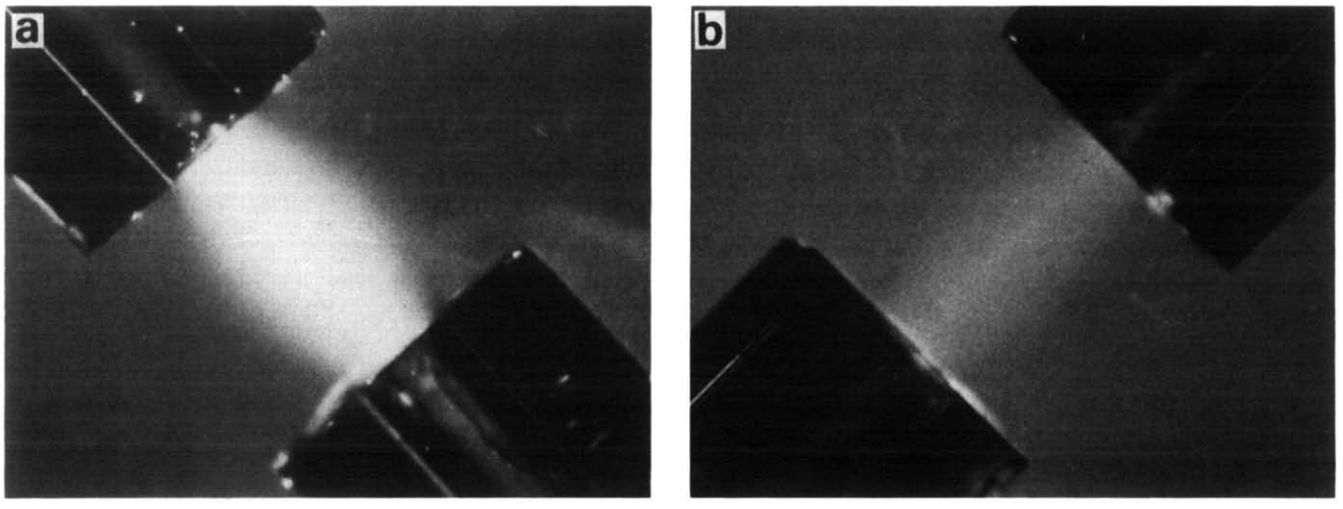

Figure 7 Photomicrographs showing the influence of elongational shear rate on sulphonated polystyrene ($g\,dl^{-1}$) in (a) fresh (rate = $1640\,s^{-1}$) and (b) salt NaCl (rate = $6080\,s^{-1}$) solutions

conformation influences behaviour in an elongational flow field. Typical photomicrograph results are presented in *Figure 7* showing the influence of salt on the level of birefringence at a particular $\dot{\varepsilon}$ with the polymer concentration above C^*, as measured in distilled water. As anticipated, the fresh water solution shows a moderate amount of retardation, since it is assumed chain entanglements limit the extensibility of the individual chains. With the addition of salt, however, the magnitude of the retardation is significantly reduced. These elongational shear rate measurements appear to parallel their associated rheological characteristics (*Figure 2*). However, the measurement of retardation as a function of $\dot{\varepsilon}$ brings out an intriguing point. These data are shown in *Figure 8*, where the retardation is plotted as a function of $\dot{\varepsilon}$. It is quite obvious that small additions of salt profoundly affect the behaviour of these chains in an elongational flow field. Even though the fresh water solution only begins to approach the limiting retardation value, the salt solution behaves as if the polymer concentration is in the dilute solution regime. That is, $\dot{\varepsilon}_c$ is observed prior to a sharp rise in retardation ending in a saturation plateau. This effect is undoubtedly due to the significant reduction of the hydrodynamic volume of the random coils culminating in extensive loss of the entanglement structure. Thus, each chain behaves as an isolated entity even at concentrations above C^*, as measured in fresh water. From this viewpoint, it is anticipated that this technique would be useful for probing the structure of individually collapsed coils in high ionic strength environments.

A careful scrutiny of $\dot{\varepsilon}_c$, measured in both fresh and salt water solutions at concentrations below C^*, reveals that higher elongational flow fields are necessary fully to elongate the coiled chains in high ionic strength environments. Direct comparison of *Figure 6* (fresh water) and *Figure 8* (salt water), for example, confirms this difference is approximately $1000\,s^{-1}$ in this instance. This difference in $\dot{\varepsilon}_c$ is directly related to the collapse of polymer chain, since a tighter bound coil would be expected to possess a shorter relaxation time and consequently an enhanced $\dot{\varepsilon}_c$. Undoubtedly, this collapse is due to primarily Debye–Hückel screening, but it could be enhanced by intramolecular hydrophobic forces. This force originates from the water structure-enhancing

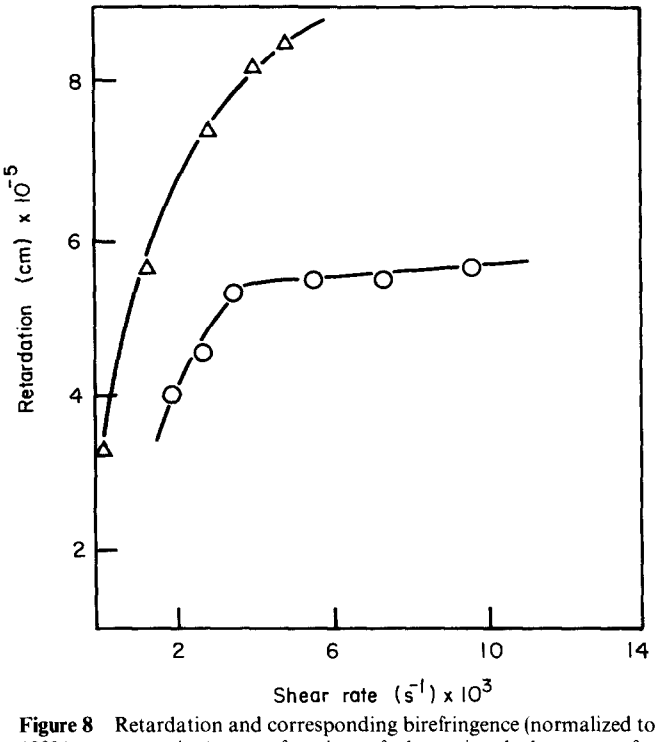

Figure 8 Retardation and corresponding birefringence (normalized to 100% concentration) as a function of elongational shear rate for sulphonated polystyrene ($1\,g\,dl^{-1}$) in distilled water (△) and 0.1 M salt solution (○)

properties of hydrocarbon-base molecules in aqueous solution[24]. Basically the hydrocarbon portions of the chain are squeezed together due to a tighter water structure. These structure-enhancing tendencies are accentuated with the addition of a number of soluble inorganic salts. In a polymer molecule, this will force the dimensions of the chain to shrink to a larger extent. An examination of the sulphonated polystyrene structure reveals that the styrenic moieties may aid in the reduced expansion of the chain in high ionic salt solutions.

Behaviour of rod-like polymers

The tendency of a polymer chain to form a coil depends to a significant extent on the flexibility of the individual chain segments. The ability to form the random conformation is sharply inhibited, and rod-like behaviour is approached as the flexibility decreases. As expected, the

physical properties of these systems can be used to detail these specific changes. A large volume of literature exists on this subject[25]. At least on a momentary basis, a rod-like conformation is obtained in an elongational flow field below C^* of the random coil. Thus, the study of the behaviour of a rod-like chain in an elongational flow field could aid in the understanding of the random coil to rod-like transition. Moreover, it is of interest to observe how rod-like polymers are influenced by $\dot{\varepsilon}$, since their properties are inherently different from a random coil.

The extracellular polysaccharide xanthan is useful in this regard, since it possesses a highly extended, rod-like conformation that maintains its viscosity characteristics in the presence of a variety of salts[26]. The viscosity–shear rate characteristics of the xanthan used in this study are shown in *Figure 9*. At low shear rates, a Newtonian plateau is observed, while moderate increases in shear produce a shear thinning region. Similar rheological properties have been found in other rod-like polymers[25]. It should be noted, based on a comparison from the literature with other rod-like polymers, that xanthan can behave as a polymeric liquid crystal[27,28]. That is, the solution properties of this material are strongly influenced by the anisotropic shape of the chain itself, and it is this factor that sharply distinguishes its behaviour from a completely random coil.

Figure 10 shows the effect of $\dot{\varepsilon}$ on the behaviour of xanthan below C^*. At low $\dot{\varepsilon}$, birefringence is visually observed over the complete field of view, while a completely dark field is present under quiescent conditions. However, a nonbirefringent region does appear along the symmetry line connecting the jets as $\dot{\varepsilon}$ is markedly increased. Clearly, this behaviour is quite different from that observed for random coils. Changing the angle of the jet with respect to the polars confirms that

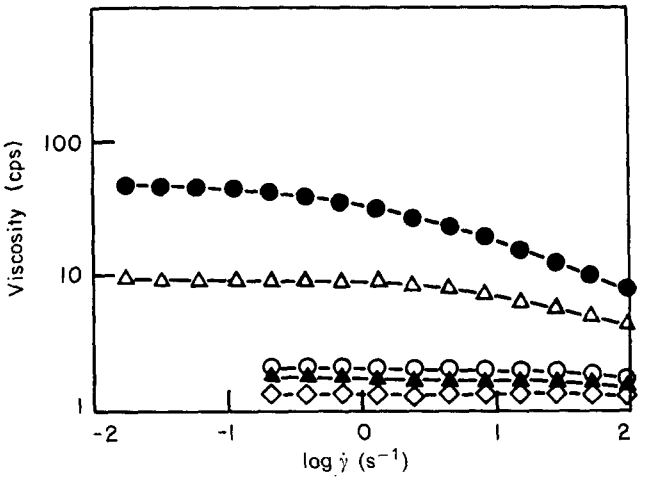

Figure 9 Viscosity–shear rate profiles of xanthan solutions in 2% sodium chloride solution (◇, 100 ppm; ▲, 125 ppm; ○, 200 ppm; △, 1000 ppm; ●, 2000 ppm)

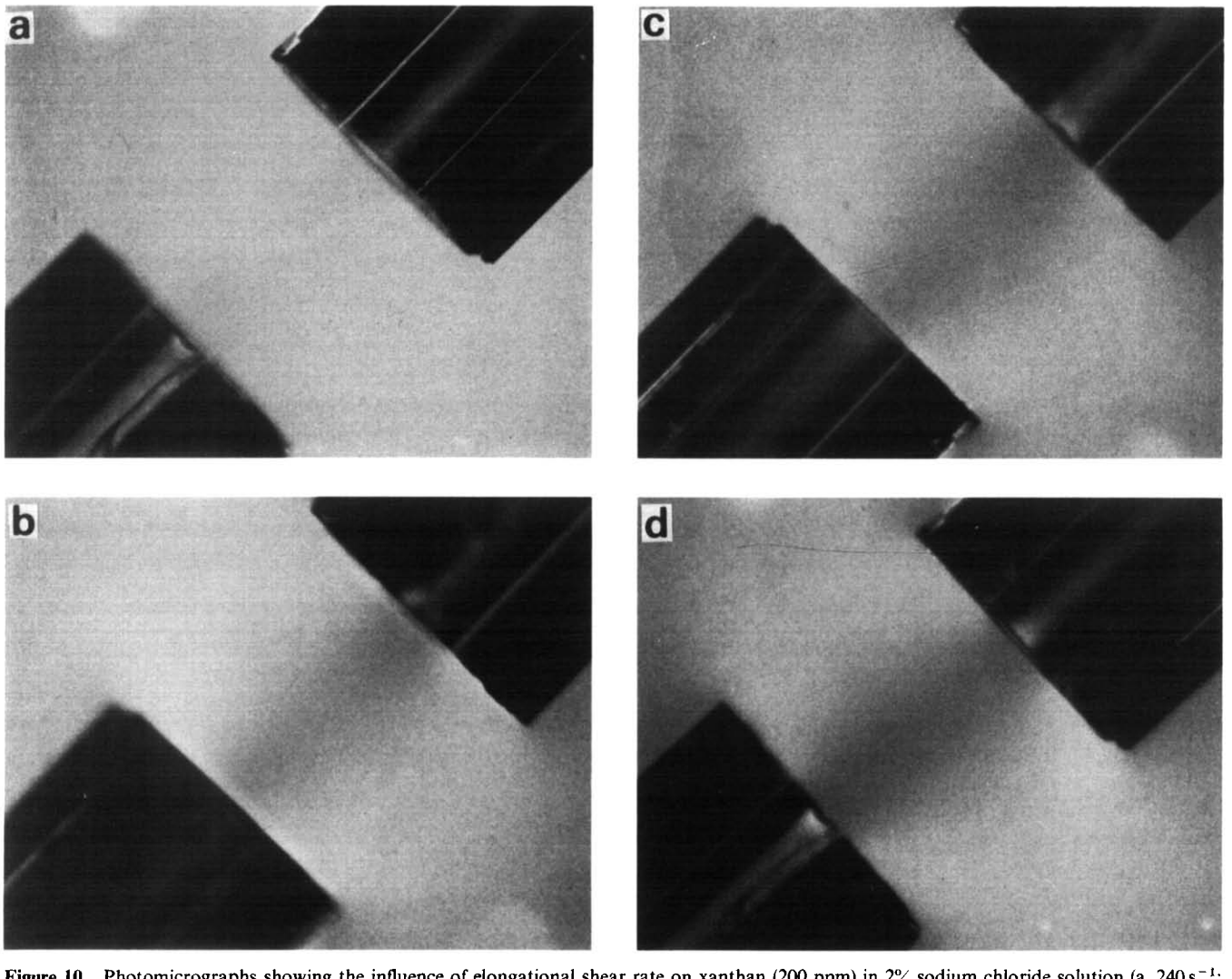

Figure 10 Photomicrographs showing the influence of elongational shear rate on xanthan (200 ppm) in 2% sodium chloride solution (a, 240 s^{-1}; b, 4800 s^{-1}; c, 9400 s^{-1}; d, 14 500 s^{-1})

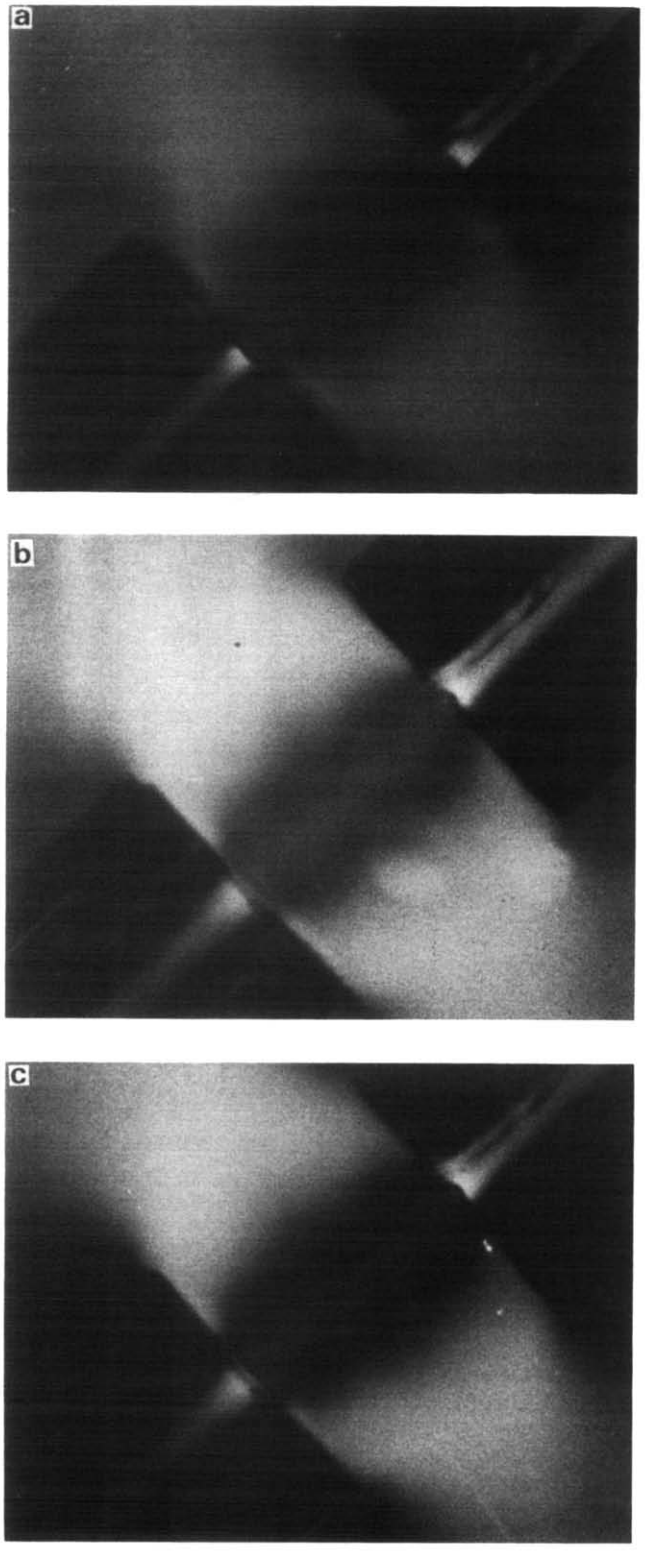

Figure 11 Photomicrographs showing the influence of elongational shear rate on xanthan (540 ppm) in 2% sodium chloride solution (a, 1300 s^{-1}; b, 11 000 s^{-1}; c, 13 100 s^{-1})

the xanthan molecules preferentially lie normal to the symmetry axis. Essentially random orientation is found in the nonbirefringent region. Therefore, it appears that below C^*, the elongational flow field readily orients the molecules outside the jet region and randomizes their orientation elsewhere at high $\dot{\varepsilon}$.

Increasing the polymer concentration to above C^* allows for a direct comparison of this orientation–disorientation process 'perturbed' by the proximity of other rod-like chains. The specific results are shown in the photomicrographs in *Figure 11*. The data parallels those given in *Figure 10*, at least at relatively moderate $\dot{\varepsilon}$. However, an additional birefringent area appears along the line connecting the centre of the jets. In this region, the axis of orientation lies parallel to this line. Thus, it is evident that the rod-like xanthan molecules are being reoriented through 90° in this flow field. The nonbirefringent area is related to this process, since it takes a finite amount of time for a majority of the rods to complete the rotation, and in doing so, all possible orientations of the rods are sampled. This 'randomization' is responsible for the lack of any observable birefringence. It is, however, interesting to note the lack of a central birefringent region below C^*. Thus, this reorientation process or transition appears to be facilitated through an intermolecular cooperative process which is readily induced through a strong elongational flow field. Further increases in concentration conform these observations, as shown in *Figure 12*. For the first time, we observe a birefringent region connecting the jet axis and little, if any, orientation outside this area at low $\dot{\varepsilon}$. The reorientation process begins to take place as $\dot{\varepsilon}$ is increased. These data strongly suggest that in this concentration range there is a marked increase in intermolecular cooperativity allowing for more facile orientation and reorientation of the rods. Indeed, this cooperativity becomes more effective as the volume fraction of anisotropic material is increased.

Figure 13 shows the effect on the elongational flow field as the polymer concentration is significantly increased. In addition to the large increase in the magnitude of the birefringence due primarily to the larger number of rod-like molecules, it is noted that the width of the non-birefringent region has shrunk to a considerable degree. Contrary to expectations, this width is not enlarged, due to the higher viscosity of this solution. Again, the width of the nonbirefringent region is consistent with the ease to which the rod-like moieties can reorient in an elongational flow field. It is apparent that it is not necessarily the viscosity of the fluid which determines this behaviour, but subtle structural features induced by the rod-like molecules within the fluid elements themselves. A detailed study of the average width of the nonbirefringent regime as a function of $\dot{\varepsilon}$ is shown in *Figure 14*. Since this length scale is a measure of the ease of this reorientation process, we find, in general, a monotonic decrease with increasing concentration.

Parallel to these results, several recent studies also have probed this interesting intermolecular cooperativity of xanthan macromolecules. The data, in all instances, can be closely related to the theoretical treatment of Flory pertaining to rigid rods in solution (ref. 25 treats this topic in some detail). The main evidence comes from the appearance of quiescent birefringence and cholesteric liquid crystal behaviour above a certain xanthan concentration[27]. These anisotropic domains are formed via intermolecular alignment of the rod-like chains. Further evidence supporting these observations comes from recent viscometric measurements at low rates of shear[28]. These results show that above a critical polymer level, the viscosity begins to fall off rapidly with increasing volume fractions of polymer. Below this level, the anticipated viscosity enhancement occurs. The maximum in the reduced-viscosity–concentration profiles correspond to the transition between isotropic and

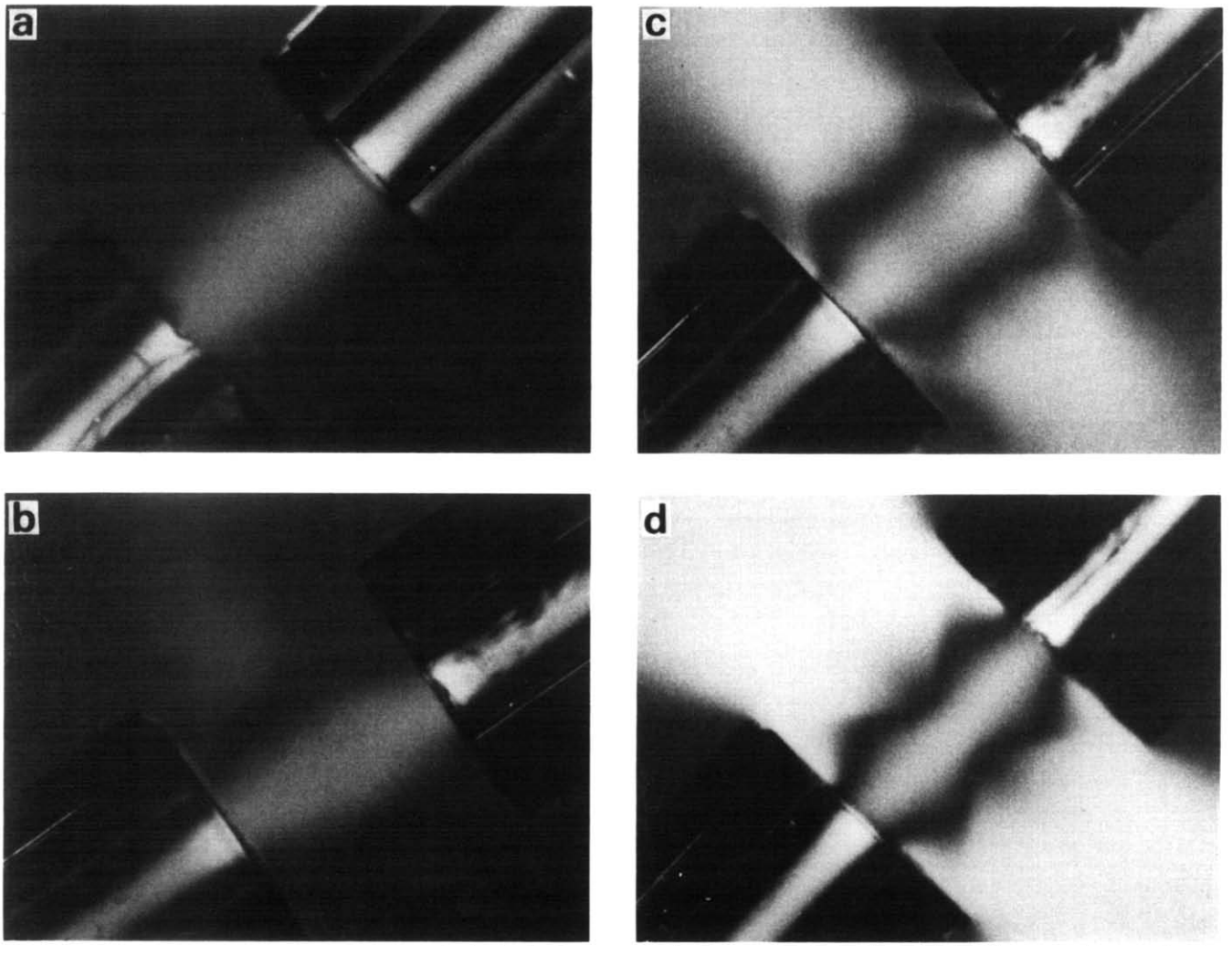

Figure 12 Photomicrographs showing the influence of elongational shear rate on xanthan (1000 ppm) in 2% sodium chloride solution (a, $140\,s^{-1}$; b, $820\,s^{-1}$; c, $3300\,s^{-1}$; d, $10050\,s^{-1}$)

anisotropic regions. It should be noted that in the anisotropic phase, the reduced viscosity is approximately identical to that found at lower polymer concentrations in the isotropic region. This mode of phase separation is quite unique in that it occurs as a consequence of the rod-like, highly anisotropic shape of the polymer chains. Attractive potentials within the chain structure itself are unnecessary in this regard. Moreover, since the anisotropic properties of these solutions are exhibited even in the absence of an external 'ordering' field, it is expected the degree of orientational order will increase if the solution is placed in an external orientational field[29]. Furthermore, it is concluded from theoretical considerations[30] that in an elongational flow, the transition between the isotropic and anisotropic phases will shift to lower concentrations and, indeed, the isotropic phase can completely disappear at sufficiently high rates of strain. Under these conditions, the isotropic solution cannot exist for most solutions of rod-like polymers possessing high axial ratios, as is shown from our elongational flow measurements both below and above C^* for xanthan.

Birefringence measurements on rod-like polymers

An investigation of the birefringence of xanthan solutions as a function of polymer level would be informative, since these measurements would quantitatively detail the ability of rod-like chain to orient in an elongational flow field. Superimposed on these results would be the strong intermolecular cooperativity effects induced in such flow environments. Typical retardation–$\dot{\varepsilon}$–concentration profiles are shown in *Figure 15*. Contrary to the results for random coils, we observe that the retardation is measurable essentially over an extensive $\dot{\varepsilon}$ range below and above C^*. This is undoubtedly attributable to the ease to which the individual rods can be oriented. As $\dot{\varepsilon}$ is increased, a saturation plateau is found at all concentrations, indicative of full alignment of the rods. However, a close examination of the curves reveals that $\dot{\varepsilon}_c$ moves to lower values with increasing volume fraction of polymer and, at least at higher polymer concentrations, with significantly higher viscosity. Thus, again the crucial factor in the orientability of these molecules lies in their ability to interact in a cooperative fashion.

These points become more clearly shown if the retardation and its associated birefringence are normalized to 100% concentration. These results are presented in *Figure 16*. The most noticeable characteristic of these curves is that the birefringence in the pleateau region is equivalent at all levels investigated. That is, if the rod-like molecules experience a sufficient $\dot{\varepsilon}$, then complete

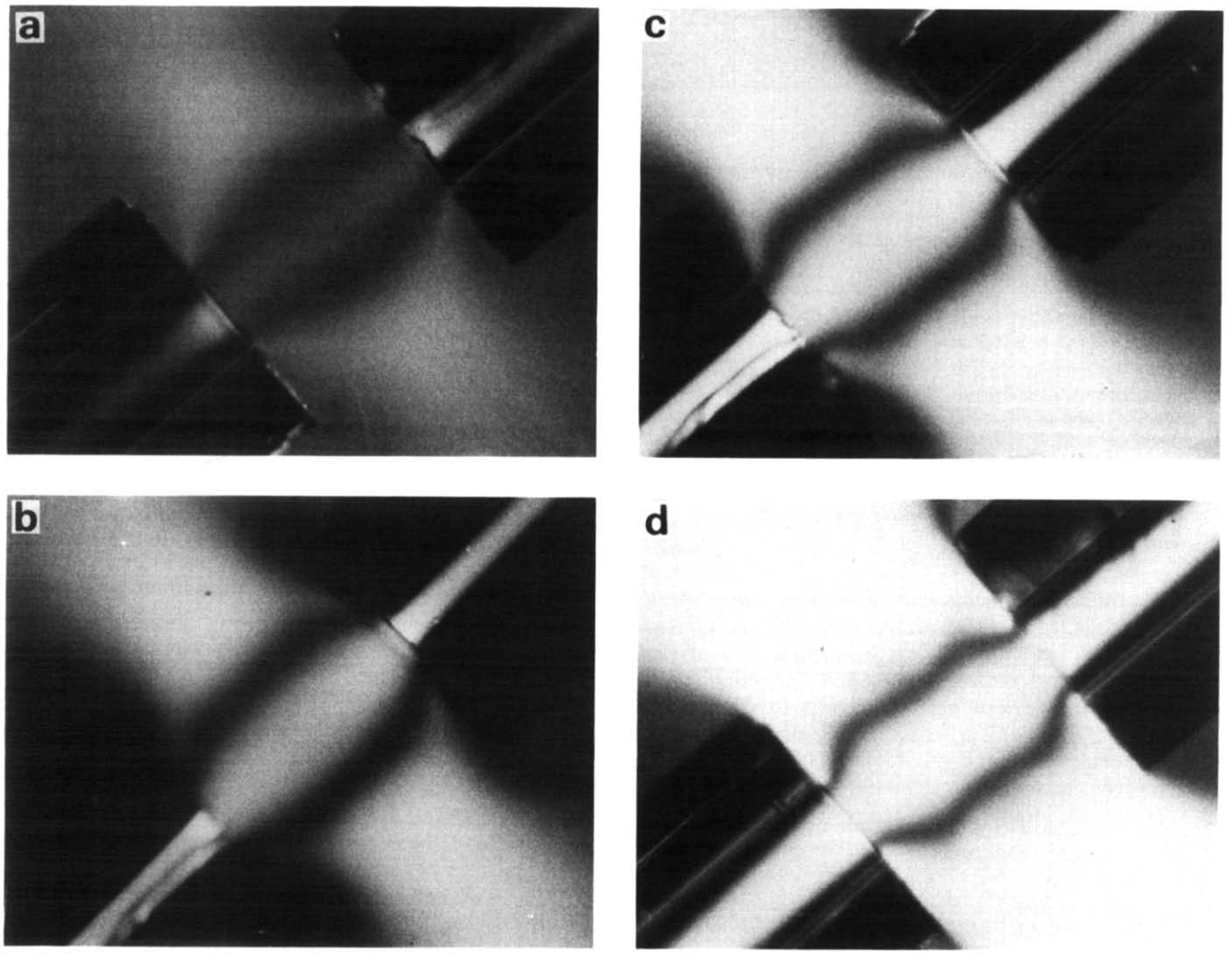

Figure 13 Photomicrographs showing the influence of elongational shear rate on xanthan (2000 ppm) in 2% sodium chloride (a, 360 s^{-1}; b, 1450 s^{-1}; c, 3200 s^{-1}; d, 10 600 s^{-1})

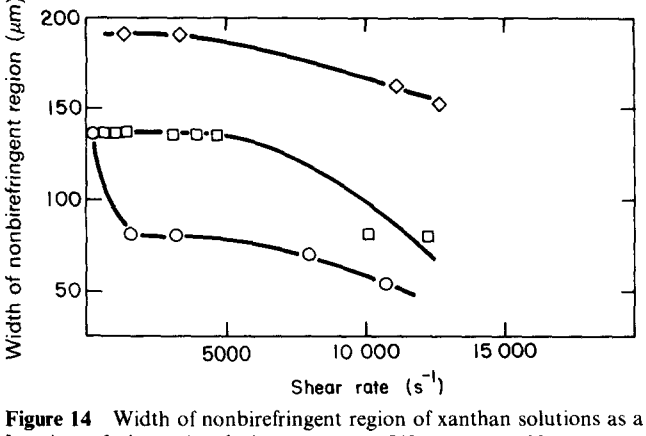

Figure 14 Width of nonbirefringent region of xanthan solutions as a function of elongational shear rate (◇, 540 ppm; □, 1000 ppm; ○, 2000 ppm)

orientation is achievable. Moreover, this orientation process is facilitated via intermolecular cooperativity induced by the elongational flow field, as noted by steepening of the curves at low $\dot{\varepsilon}$ with marked increases in the volume fraction of polymer in solution.

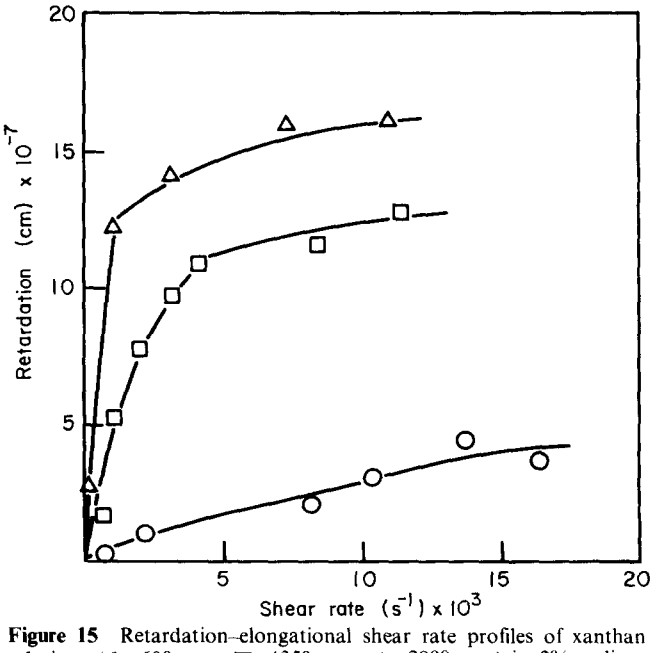

Figure 15 Retardation–elongational shear rate profiles of xanthan solutions (○, 600 ppm; □, 1350 ppm; △, 2000 ppm) in 2% sodium chloride

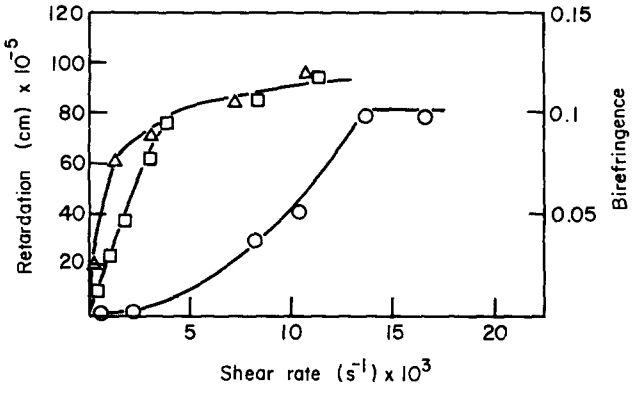

Figure 16 Retardation and corresponding birefringence (normalized to 100% concentration) as a function of elongational shear rate for xanthan solutions (○, 600 ppm; □, 1350 ppm; △, 2000 ppm) in 2% sodium chloride

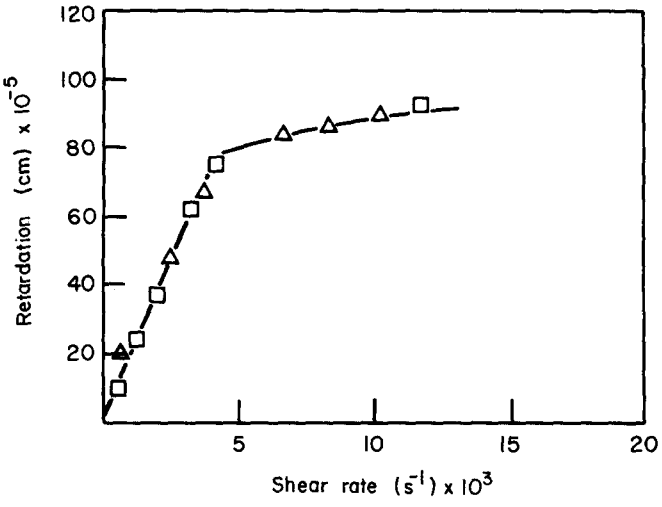

Figure 17 Dependence of retardation, normalized to 100% concentration, on elongational shear rate for xanthan (1350 ppm) in sodium chloride solutions: □, 2%; △, 4%

Influence of salt

Finally, the ability to induce the random coil to rod-like transition greatly depends on the polymer concentration and ionic strength. Contrary to these results, we find that the rigid rod xanthan behaviour in an elongational flow field is unaffected by the presence of salt. A typical example is shown in *Figure 17*. A comparison of the birefringence–$\dot{\varepsilon}$ curves at equivalent polymer concentrations and various salt levels (up to 4% NaCl) confirms that the data are completely superimposable. These trends parallel the rheological characteristics of xanthan, which are not significantly modified with changes in ionic strength.

CONCLUSION

In this paper, we have shown that the high elongational characteristics of the flow field generated in an opposing jet device can be used to probe the molecular characteristics of a variety of polymeric structures. In particular, structural features of an individual chain, i.e. inherent flexibility, interaction with other chains and the solvent environment in which it is dissolved, have a major impact on the response of the polymer system to an elongational flow.

A rod-like chain, such as xanthan, is easily oriented at all $\dot{\varepsilon}$. However, a closer examination of the data confirms that the ability of these rod-like macromolecules to orient and/or reorient in an elongational flow field is facilitated through cooperative intermolecular interactions. Furthermore, it is apparent that $\dot{\varepsilon}$ is able to induce this order–disorder transition at least above C^*. Thus, xanthan benefits greatly from its inflexible structure in its ability to respond to an elongational flow field.

A random coil (sulphonated polystyrene) clearly parallels the theoretical predictions. In dilute solution, the individual coil will rapidly expand its dimensions to its fullest extent after $\dot{\varepsilon}_c$ is reached. In this state, the random coil can be described as a rod-like entity; however, this exists for a relatively short moment, since entropic considerations dictate the more stable conformation. As C^* is approached, entanglements begin to dominate elongational behaviour. Our results in this concentration range confirm that it is quite easy to orient segments of overlapping chains, but complete chain extension can only be approached. It is noted, however, that complete extension of the polyelectrolyte may be possible at concentrations above C^*, if the ionic strength of the solution is increased. In this instance, it appears that the hydrodynamic volume of the coils shrink to a sufficient extent that chain overlap becomes an ineffective interaction mode. A direct consequence of this reduction is that the collapsed coils require a larger $\dot{\varepsilon}_c$ for complete extension (i.e. more tightly coiled conformation) as compared with coils in a very low ionic strength solution.

REFERENCES

1 Flory, P. J. 'Principles of Polymer Chemistry', Cornell Univ. Press, Ithaca, New York, 1967
2 Perkins, W. G. and Porter, R. S. *J. Mater. Sci.* 1981, **16**, 1458
3 Brigg, D. M. *Polym. Eng. Sci.* 1976, **16**, 725
4 Elyashevich, G. K. *Adv. Polym. Sci.* 1982, **43**, 205
5 Ohta, T. *Polym. Eng. Sci.* 1983, **23**, 697
6 Peng, S. T. J. and Landel, R. F. *J. Appl. Phys.* 1976, **47**, 4255
7 Balmer, R. T. and Hochschild, D. J. *J. Rheol.* 1978, **22**, 165
8 Lumley, J. L. *Phys. Fluids* 1977, **20**, S64
9 Peterlin, A. *J. Polym. Sci.* 1966, **287**, B4
10 Lumley, J. L. in 'Symposia Mathematica', Academic Press, New York, 1972, **9**, 315
11 De Gennes, P. G. *J. Chem. Phys.* 1974, **60**, 5030
12 Marrucci, G. *Polym. Eng. Sci.* 1975, **15**, 229
13 Pope, D. P. and Keller, A. *Colloid Polym. Sci.* 1978, **256**, 751
14 Farrell, C. J., Keller, A., Miles, M. J. and Pope, D. P. *Polymer* 1980, **21**, 1292
15 Gardner, K., Pike, E. R., Miles, M. J., Keller, A. and Tanaka, K. *Polymer* 1982, **23**, 1435
16 Miles, M. J., Tanaka, K. and Keller, A. *Polymer* 1983, **24**, 1081
17 Holzwarth, G. *Carbohydr. Res.* 1978, **66**, 173
18 Wiener, O. *Abhandl. Saechs. Akad. Wiss. Leipzig, Math. Physik. K1.* 1912, **32**, 575
19 Jamieson, A. M., Southwich, J. G. and Blackwell, J. *J. Faraday Symp. Chem. Soc.* 1983, **18**, 131
20 Graessley, W. W. *J. Chem. Phys.* 1967, **47**, 1942
21 DeWitt, T. W., Markovitz, H., Padden, F. J. and Zapas, L. J. *J. Colloid Sci.* 1955, **10**, 174
22 Graessley, W. W., Hazleton, R. L. and Lindeman, L. R. *Trans. Soc. Rheol.* 1967, **11**, 267
23 Tsvetkov, V. N. *Polym. Rev.* 1964, **6**, 563
24 Ben-Naim, A. 'Hydrophobic Interactions', Plenum Press, New York and London, 1980
25 Wissbrun, K. F. *J. Rheol.* 1981, **25**, 619
26 Jeanes, A., Pittsley, J. E. and Senti, F. R. *J. Appl. Polym. Sci.* 1961, **5**, 519
27 Rinaudo, M. and Milas, M. *Carbohydr. Polym.* 1982, **2**, 264
28 Milas, R. and Rinaudo, M. *Polym. Bull.* 1983, **10**, 271
29 Khokhlov, A. R. and Semenov, A. N. *Macromolecules* 1982, **15**, 1272
30 Maissa, P., Ten Bosch, A. and Sixou, P. *J. Polym. Sci., Polym. Lett. Edn.* 1983, **21**, 757